# Transport Numbers of Singly-, Doubly- and Triply-Charged Cations in Porous Glasses

**L. E. Ermakova[a, *, **], A. S. Kuznetsova[a, b], and T. V. Antropova[b]**

*[a] St. Petersburg State University, St. Petersburg, 199034 Russia*
*[b] Grebenshchikov Institute of Silicate Chemistry, Russian Academy of Sciences, St. Petersburg, 199034 Russia*
*\*e-mail: ermakova3182@yandex.ru*
*\*\*e-mail: l.ermakova@spbu.ru*

**Abstract**—Transport numbers of sodium, nickel, and lanthanum counterions have been studied in microporous (average pore radius is $r = 2$–$3.4$ nm) and macroporous ($r = 16$–$27$ nm) magnetite-free glasses and those containing magnetite in their matrices. It has been found that, in the case of microporous glasses, the relation between the transport numbers of the studied cations is primarily governed by the structure of secondary silica in pore channels. For membranes prepared from macroporous glasses, the transport numbers of the cations in the pore space depend on the surface charge magnitude and the structure of the electrical double layer.

## INTRODUCTION

Transport numbers of ions are important characteristics of membrane systems, and the knowledge of their values is necessary for understanding the relation between the mechanisms of transmembrane transport processes induced by external fields and the structural and electrosurface parameters of membranes having different chemical compositions. It is also of interest to analyze the transport characteristic of porous glasses (PGs) as depending on counterion charges. These glasses may be used as membranes for separating liquid media and as functional elements of microanalytical systems (microfluid chips, electroosmotic pumps, etc.) [1–7]. Selectivity and other working characteristics of such membrane systems are related to the transport numbers and mobilities of ions in membrane pore space.

PGs obtained from sodium borosilicate glass, as well as hematite-containing PGs, the structural and electrokinetic characteristics of which were previously investigated in solutions of different electrolytes [8–12], were selected as the objects for this study. Their transport characteristics were compared in solutions of sodium, nickel, and lanthanum chlorides. This made it possible to analyze the influence of the charges of the counterions (cations) on the properties of such membrane systems, which have a negative surface charge, in the presence of the same coion—chlorine ion.

## EXPERIMENTAL

PGs with average pore radius $r = 1.3$ nm (microporous, MIP glasses) were obtained at the Grebenshchikov Institute of Silicate Chemistry, Russian Academy of Sciences, from monolithic two-phase glasses by the through acidic (3 M hydrochloric or nitric acid, 100°C) leaching of thermotreated two-phase sodium borosilicate glass with a two-frame structure [10]. According to the synthesis conditions, the glass had the following composition (mol %): $Na_2O$, 8; $B_2O_3$, 22; and $SiO_2$, 70. Macroporous (MAP) 8V-NT glasses with average pore radii of 19.7–25.5 nm were prepared via an alkaline treatment of MIP glasses with a 0.5 M KOH solution at room temperature. Silica content in the obtained PGs was more than 95%; i.e., they are typical high-silica channel nanostructures. The bulk porosity (ratio between the pore volume and the total membrane volume) was 0.23–0.24 and 0.51–0.61 for MIP and MAP glasses, respectively.

While the transport numbers were measured, the average pore radius of 8V-NT MIP membranes increased to 2–3.4 nm due to the removal of dissolved secondary silica from the pore space. For 8V-NT MAP membranes, the increase in the pore channels size occurred due to the slight dissolution of the silica matrix and was small; the $r$ values grew to 20–27 nm [12].

Hematite was incorporated by adding iron oxide to the initial batch mixture when the glass was melted. The resulting monolithic glass (Fe-4-5) with an iron

oxide content of 11.16 mol % was subjected to thermal treatment for phase separation; then, it was used to obtain the micro- and macroporous glasses by the acidic leaching and alkaline treatment [9, 12]. The volume-average iron content was 21.1 ± 1 wt % for freshly prepared micro- and macroporous membranes and 15.6 wt % for membranes exposed in electrolyte solutions for a long time [12]. The average pore radius of Fe-4-5 MIP membranes was 1.8–1.9 nm, while, for Fe-4-5 MAP membranes, it was 16.5–18.1 nm. The bulk porosities of MIP and MAP samples were 0.19 and 0.45, respectively. After the long-term contact with electrolytes, the average pore radii of MIP and MAP samples increased to 2.4–3 and 17–19 nm, respectively [9, 12].

The membranes of all types used to measure the ion transport numbers had shapes of disks with a thickness and a diameter of nearly 1 and 30 mm, respectively. The preparation conditions of the membranes are presented in their denotations.

Transport number $n_i$ of an $i$th ion is the fraction of electricity that is transported by the $i$-type ions relative to the total quantity of electricity. Molar transference number $t_i$ of the $i$th ion is the number of moles of the $i$-type ions transported with one faraday of electricity through the cross section of a conductor in the direction of electric current [13]. When using this definition, it is necessary to take into account that the molar transference number of anions is negative. The following relation is valid for the transport numbers:

$$\sum_i n_i = \sum_i z_i t_i = 1, \tag{1}$$

where $z_i$ is the ion charge with allowance for its sign. Note that for an 1 : 1 electrolyte, the $n_i$ and $t_i$ values coincide with one another; for anions—with an accuracy of the sign.

Assuming that the molar transference numbers for ions of both signs are positive values, the following expression may be written:

$$\sum_i |z_i| t_i = 1. \tag{2}$$

The membrane potential method is one of the methods used to determine experimentally the molar transference numbers. The membrane potential was measured using a concentration transfer circuit, the emf of which was equal to $E$. The scheme of the concentration transfer circuit was as follows:

| Ag/AgCl reversible electrode | Solution 1 $a_{\pm(1)}$ | Membrane | | Solution 2 $a_{\pm(2)}$ | Ag/AgCl reversible electrode |
|---|---|---|---|---|---|
| Electrode potential | | $\varphi_D^I$ | $\varphi_D^{II}$ | | Electrode potential |
| Membrane diffusion potential | | | | | |

Here, $\varphi_D^I$ and $\varphi_D^{II}$ are the Donnan potentials and $a_{\pm(1)}$ and $a_{\pm(2)}$ are the average activities of the electrolyte solutions brought in contact with the membrane. The measurements are commonly performed at $a_{\pm(1)}/a_{\pm(2)} \approx 2$.

The value of $E$ is the sum of membrane diffusion potential $E_M$ and the difference of the electrode potentials. When using solutions of chlorides as electrolytes and reversible silver chloride electrodes, measured electrode potential difference $\Delta E_E$ comprises concentration potential $E_C$ and electrode asymmetry potential $E_{AS}$.

Assuming that, within a rather narrow concentration range, the transport numbers of ions in a membrane weakly depend on electrolyte concentration, we used the following equation that relates the values of $E_M$ and $t_-$, i.e., the transport numbers of Cl$^-$ ions (we take that $t_- > 0$), which, in the case of negatively charged PGs, are coions [13]:

$$E_M = -\frac{RT}{z_+ F}\left[\ln\frac{a_{+(2)}}{a_{+(1)}} - (z_+ - z_-)t_- \ln\frac{a_{\pm(2)}}{a_{\pm(1)}}\right]. \tag{3}$$

In our case, the electrode potential difference has the following form:

$$\Delta E_E = E_C + E_{AS} = \frac{RT}{z_- F}\ln\frac{a_{-(2)}}{a_{-(1)}} + E_{AS}, \tag{4}$$

where $a_{+(1)}$ and $a_{+(2)}$ are the activities of counterions, $a_{-(1)}$ and $a_{-(2)}$ are the activities of coions, and $a_{\pm(1)}$ and $a_{\pm(2)}$ are the average activities of the electrolyte on different sides of the membrane. Assuming that, in the studied concentration range, $\frac{a_{+(2)}}{a_{+(1)}} \cong \frac{a_{-(2)}}{a_{-(1)}} \cong \frac{a_{\pm(2)}}{a_{\pm(1)}}$, we obtain

$$E_M + E_C = \frac{RT(z_+ - z_-)}{z_+ z_- F}\ln\frac{a_{+(2)}}{a_{+(1)}}(1 + z_- t_-). \tag{5}$$

**Table 1.** Degrees of hydrolysis and concentrations of hydrolyzed forms of nickel and lanthanum cations

| $I$, mol/L | NiCl$_2$ | | | LaCl$_3$ | | |
|---|---|---|---|---|---|---|
| | $C$, mol/L | $h$ | $C_K$, mol/L | $C$, mol/L | $h$ | $C_K$, mol/L |
| $3 \times 10^{-1}$ | $1.00 \times 10^{-1}$ | $1.10 \times 10^{-5}$ | $1.10 \times 10^{-6}$ | $5 \times 10^{-2}$ | $2.00 \times 10^{-5}$ | $1.00 \times 10^{-6}$ |
| $10^{-1}$ | $3.33 \times 10^{-2}$ | $1.90 \times 10^{-5}$ | $6.32 \times 10^{-7}$ | $1.67 \times 10^{-2}$ | $3.46 \times 10^{-5}$ | $5.78 \times 10^{-7}$ |
| $10^{-2}$ | $3.33 \times 10^{-3}$ | $6.01 \times 10^{-5}$ | $2.00 \times 10^{-7}$ | $1.67 \times 10^{-3}$ | $1.09 \times 10^{-4}$ | $1.82 \times 10^{-7}$ |
| $10^{-3}$ | $3.33 \times 10^{-4}$ | $1.90 \times 10^{-4}$ | $6.32 \times 10^{-8}$ | $1.67 \times 10^{-4}$ | $3.46 \times 10^{-4}$ | $5.78 \times 10^{-8}$ |
| $10^{-4}$ | $3.33 \times 10^{-5}$ | $6.01 \times 10^{-4}$ | $2.00 \times 10^{-8}$ | $1.67 \times 10^{-5}$ | $1.09 \times 10^{-3}$ | $1.82 \times 10^{-8}$ |

Then, in the case of a $z_+ : z_-$ electrolyte, the expression for the molar transference number of a cation acquires the following form:

$$t_+ = \frac{1}{z_+} n_+ = \frac{z_-(\Delta E_E - E_{AS})}{\frac{(z_+ - z_-)RT}{F} \ln( a_{\pm(2)}/a_{\pm(1)})}. \quad (6)$$

In the case of a 1 : 1 electrolyte, Eq. (6), yields the following well-known expression for the cation transport number in a membrane:

$$t_+ = n_+ = \frac{\Delta E_E - E_{AS}}{\frac{2RT}{F} \ln( a_{\pm(1)}/a_{\pm(2)})}. \quad (7)$$

In addition, the transport numbers may be expressed via the ionic equivalent conductivities of electrolyte cations and anions $\lambda_i$ or mobilities $U_i$ of the ions ($\lambda_i = FU_i$) [14, 15]:

$$n_i = \lambda_i \Big/ \sum_i \lambda_i = U_i \Big/ \sum_i U_i. \quad (8)$$

The transport numbers of cations in a solution ionic strength range of $I \leq 0.1$ M were calculated using the ratio between specific conductivities $\kappa_V$ of the solutions on different sides of a membrane rather than the ratio between the average activities of these solutions. The $\kappa_V$ values were determined using alternating current with a frequency of 1 kHz (E7-21 immittance meter). The membrane potentials were measured with a Fluke 8846A/Su multimeter in a flow-through cell [16] at $22 \pm 2°C$ and neutral pH values (5.6–5.7).

Solutions were prepared in deionized water ($\kappa_V \leq 1.5 \times 10^{-6}$ $\Omega^{-1}$ cm$^{-1}$, Aqualab AL Plus water-purification system) using reagents of the extra-pure or reagent grade. The error in the determination of the $n_+$ values was no larger than $\pm 0.02–0.03$.

## RESULTS AND DISCUSSION

The studies and comparison of the transport characteristics for the micro- and macroporous glasses of different compositions in solutions of sodium, nickel, and lanthanum chlorides were performed at the same ionic strengths $I = 0.5\sqrt{\sum_i z_i^2 C_i}$ ($10^{-4}–10^{-1}$ M). This provided constant values of diffusion layer thickness and almost equal degrees of electrical double layer (EDL) overlap in the pore channels of the membranes at close values of the average pore radius.

Let us initially consider the characteristics of the studied cations in free solutions of the corresponding electrolytes. It is known that actually no hydrolysis processes occur in solutions of electrolytes of the NaCl type. In solutions of nickel and lanthanum chlorides, hydrolyzed forms of cations may be formed; therefore, degree of hydrolysis $h$ was determined proceeding from the parameters of the first step of the hydrolysis, i.e., dissociation constants $K_D$ of corresponding hydroxo complexes, with these constants being equal to $10^{-3.08}$ and $10^{-3.3}$ for nickel and lanthanum, respectively [17]:

$$h = \sqrt{K_H/C} = \sqrt{K_W/K_D C}, \quad (9)$$

where $K_H$ is the hydrolysis constant, $K_W$ is the ionic product of water, and $C$ is the electrolyte molar concentration. For the studied range of electrolyte ionic strengths, the values of $h$ and the concentrations of hydrolyzed forms of nickel NiOH$^+$ and lanthanum LaOH$^{2+}$ cations ($C_K = Ch$) are listed in Table 1. It can be seen that, throughout the studied range of liquid phase compositions, the concentrations of nickel and lanthanum hydroxo complexes are 4–5 orders of magnitude lower than the electrolyte concentrations, and their influence on the properties of the membrane systems may be ignored.

The radii of the studied cations according to Goldschmidt $r_G$ [17], Belov and Bokii $r_B$ [18], and Shannon and Prewitt $r_{Sh}$ [19], as well as their equivalent conductivities at infinite dilution $\lambda_0$ (at 25°C) [20], are summarized in Table 2. The same table shows the Stokes radii of these ions

$$r_{St} = \frac{|z_i| F^2}{6\pi \eta N \lambda_0} \quad (10)$$

and radii $r_{cor}$ determined taking into account the corrections to the Stokes law [21].

**Table 2.** Structural and electrochemical characteristics of sodium, nickel, and lanthanum cations

| Parameter | Na$^+$ | Ni$^{2+}$ | La$^{3+}$ |
|---|---|---|---|
| $r_G$, nm | 0.098 | 0.078 | 0.122 |
| $r_B$, nm | 0.098 | 0.074 | 0.104 |
| $r_{Sh}$, nm | 0.102 | 0.069 | 0.103 |
| $\lambda_0$, $\Omega^{-1}$ g-equiv$^{-1}$ cm$^2$ | 50.1 | 54 | 69.7 |
| $r_{St}$, nm | 0.184 | 0.341 | 0.396 |
| $r_{cor}$, nm | 0.33 | 0.43 | 0.46 |
| $(V - V_C)$, nm$^3$ | 0.146 | 0.331–0.332 | 0.403–0.406 |
| $k$ | 5 | 11 | 13–14 |

The values of $r_{cor}$ were used to calculate volumes $V$ of the hydrated ions and numbers $k$ of water molecules in the hydration shells:

$$k = (V - V_C)/V_{H_2O}, \tag{11}$$

where $V_C$ denotes the ion volumes found from the values of $r_G$, $r_B$, and $r_{Sh}$ (ranges of $(V - V_C)$ values are presented), while water molecule volume $V_{H_2O}$ was taken to be 0.03 nm$^3$ [21]. The data obtained are shown in Table 2. It is seen that the methods used to determine the proper sizes of the cations have actually no effect on the number of water molecules in a hydration shell.
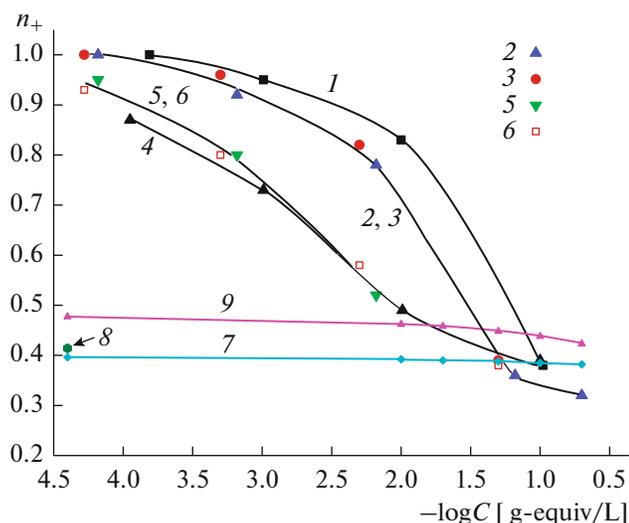
The transport numbers calculated for the cations from the membrane potentials measured for the studied systems, as well as the published transport numbers in free solutions of the studied electrolytes (the points presented in the plots for the most diluted solutions correspond to the infinite dilution) [20], are shown in Figs. 1–6.

Since all reference electrochemical data on univalent and multivalent ions in solutions are presented at the same equivalent concentrations, i.e., as calculated per one charge, analogous dependences were plotted for the transport numbers in the PGs (Figs. 1, 2). It is seen that ordinary dependences of $n_+$ on electrolyte concentration are observed in all cases; i.e., in the pore space, the transport numbers of counterions having different charge values increase with dilution to reach unity in the most diluted solutions for all MIP glasses. The membranes become ideally selective, because the degree of EDL overlapping is, in this case, high in the pore space; i.e., the values of electrokinetic radius $\kappa r$ ($\kappa = \left[ \left( F^2 \sum_i z_i^2 C_i \right) \Big/ \varepsilon \varepsilon_0 RT \right]^{1/2}$ is the Debye parameter) in the studied MIP glasses are within a range of 0.08–0.14. Hence, coions actually do not penetrate into the membranes, and their concentration is several orders of magnitude lower than the concentration of counterions [22].

At the same concentration of an equilibrium solution within a range of $1.8 \times 10^{-4} < C < 1 \times 10^{-1}$ g-equiv/L, the maximum values of $n_+$ are observed for Na$^+$ ions in MIP glasses of both types. In the most concentrated (0.1 M) NaCl solution, the transport numbers of Na$^+$ ions in



**Fig. 1.** Dependences of cation transport numbers on equivalent concentrations of electrolytes for 8V-NT porous glasses: (*1*) 8V-NT (3 M HCl) MIP, NaCl; (*2*) 8V-NT (3 M HCl) MIP, NiCl$_2$; (*3*) 8V-NT MIP, LaCl$_3$; (*4*) 8V-NT (3 M HNO$_3$, 0.5 M KOH) MAP, NaCl; (*5*) 8V-NT (3 M HCl, 0.5 M KOH) MAP, NiCl$_2$; (*6*) 8V-NT (3 M HNO$_3$, 0.5 M KOH) MAP, LaCl$_3$; and (*7*, *8*, *9*) free solutions of NaCl, NiCl$_2$, and LaCl$_3$, respectively.
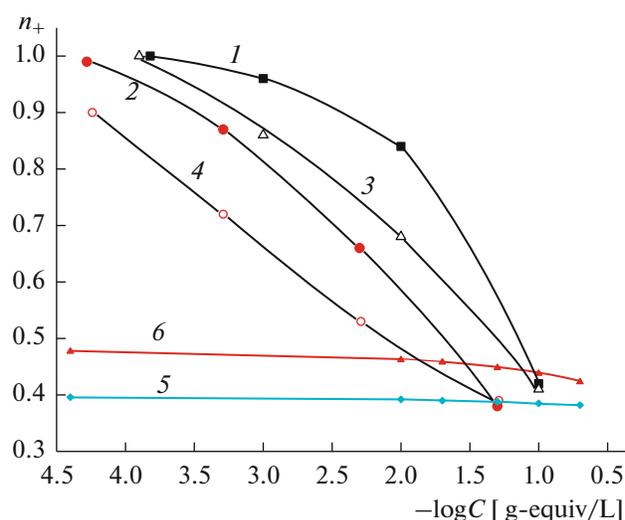


**Fig. 2.** Dependences of cation transport numbers on equivalent concentrations of electrolytes for Fe-4-5 porous glasses. (*1*) Fe-4-5 (3 M HCl) MIP, NaCl [9]; (*2*) Fe-4-5 (3 M HCl) MIP, LaCl$_3$; (*3*) Fe-4-5 (3 M HCl, 0.5 M KOH) MAP, NaCl [9]; (*4*) Fe-4-5 (3 M HCl, 0.5 M KOH) MAP, LaCl$_3$; and (*5*, *6*) free solutions of NaCl and LaCl$_3$, respectively.
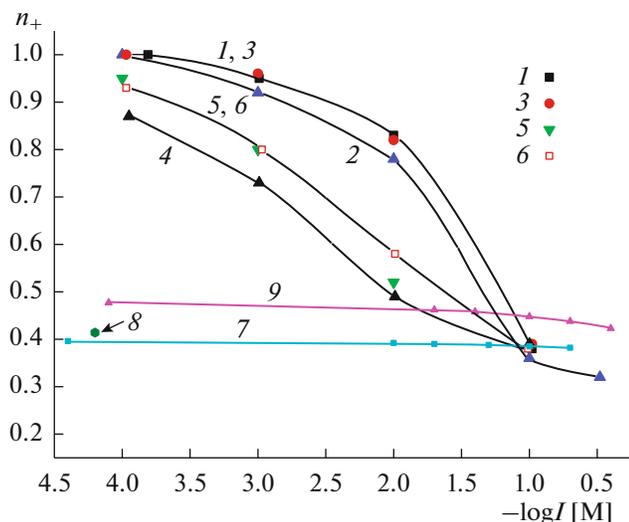
**Fig. 3.** Dependences of cation transport numbers on electrolyte ionic strengths for 8V-NT porous glasses. (*1*) 8V-NT (3 M HCl) MIP, NaCl; (*2*) 8V-NT (3 M HCl) MIP, NiCl$_2$; (*3*) 8V-NT MIP (3 M HCl), LaCl$_3$; (*4*) 8V-NT (3 M HNO$_3$, 0.5 M KOH) MAP, NaCl; (*5*) 8V-NT (3 M HCl, 0.5 M KOH) MAP, NiCl$_2$; (*6*) 8V-NT (3 M HNO$_3$, 0.5 M KOH) MAP, LaCl$_3$; and (*7, 8, 9*) free solutions of NaCl, NiCl$_2$, and LaCl$_3$, respectively.
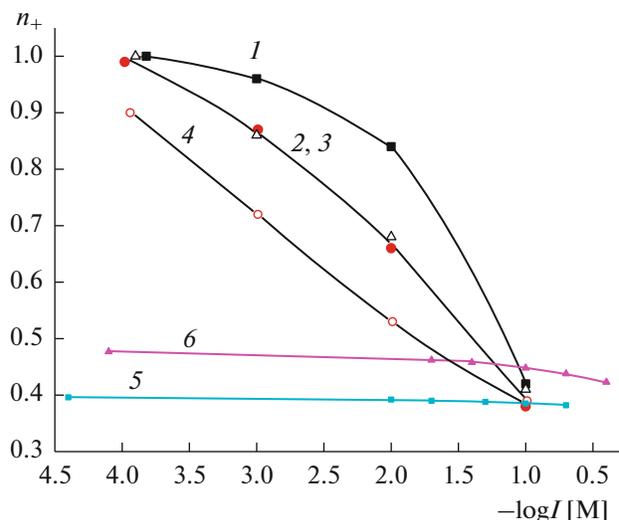


**Fig. 4.** Dependences of cation transport numbers on electrolyte ionic strengths for Fe-4-5 porous glasses. (*1*) Fe-4-5 (3 M HCl) MIP, NaCl [9]; (*2*) Fe-4-5 (3 M HCl) MIP, LaCl$_3$; (*3*) Fe-4-5 (3 M HCl, 0.5 M KOH) MAP, NaCl [9]; (*4*) Fe-4-5 (3 M HCl, 0.5 M KOH) MAP, LaCl$_3$; and (*5, 6*) free solutions of NaCl and LaCl$_3$, respectively.
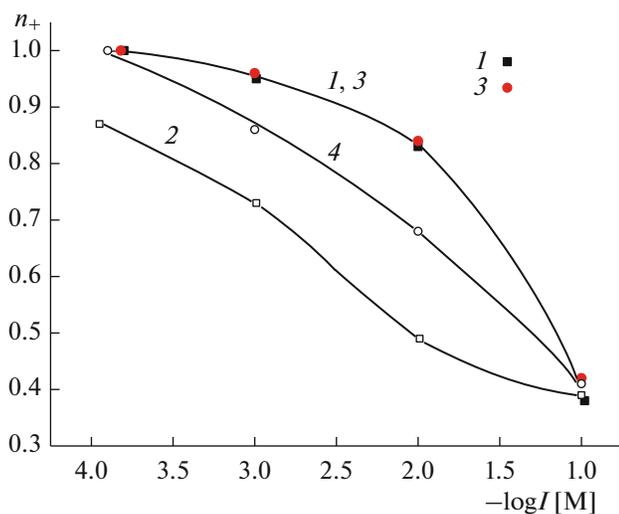


**Fig. 5.** Dependences of cation transport numbers on ionic strength of NaCl solutions: (*1*) 8V-NT (3 M HCl) MIP, (*2*) 8V-NT (3 M HNO$_3$, 0.5 M KOH) MAP, (*3*) Fe-4-5 (3 M HCl) MIP [9], and (*4*) Fe-4-5 (3 M HCl, 0.5 M KOH) MAP [9].
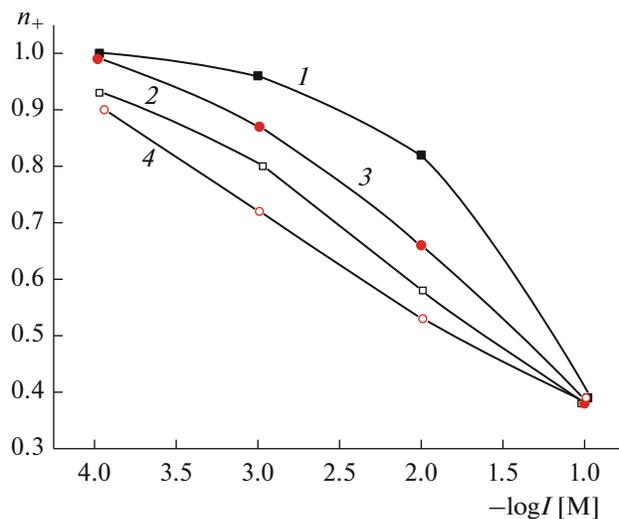


**Fig. 6.** Dependences of cation transport numbers on ionic strength of LaCl$_3$ solutions: (*1*) 8V-NT (3 M HCl) MIP, (*2*) 8V-NT (3 M HNO$_3$, 0.5 M KOH) MAP, (*3*) Fe-4-5 (3 M HCl) MIP, and (*4*) Fe-4-5 (3 M HCl, 0.5 M KOH) MAP.

micro- and macroporous 8V-NT membranes almost coincide with the value corresponding to a free solution, while, for Fe-4-5 membranes, they are somewhat higher (0.41−0.42 vs. 0.385 in the solution).

In free solutions, the passage from univalent Na$^+$ ions to divalent Ni$^{2+}$ ions leads to only a slight increase

in the transport number (Fig. 1), since the equivalent conductivity and, hence, the ion mobility also remain almost unchanged (Table 1), because, in addition to an increase in the charge, the size of the ion hydration shell rises (the $k$ value increases twofold). As the cation charge further grows, i.e., upon the passage to La$^{3+}$ ions, the size of the hydration shell changes not so sig-

nificantly; therefore, the equivalent conductivity, mobility, and transport number increase as compared with sodium and nickel ions.

At equilibrium concentrations lower than $1.8 \times 10^{-4}$ g-equiv/L, the transport number of sodium ions in the pore space of 8V-NT MIP membranes is higher than those of the multivalent ions, with the $n_+$ values for $Ni^{2+}$ and $La^{3+}$ ions coinciding with one another within the experiment error (Fig. 1, curves *1–3*). This suggests a substantial decrease in the mobility of $Ni^{2+}$ and $La^{3+}$ ions, the sizes of which are larger than the size of a $Na^+$ ion, in the MIP glass pores, which contain secondary silica. It should also be noted that, at the same equivalent concentration, the molar concentration diminishes upon the passage from a 1 : 1 to 2 : 1, and further to 3 : 1 electrolytes, thereby increasing the swelling degree of secondary silica and a decreasing the mobility of multivalent cations in the pores. Seemingly, it is also of importance that, at nearly the same sizes of the cations, the interaction of di- and trivalent ions with the surface of the pore channels is stronger due to the stronger Coulomb attraction to the negatively charged silica surface. The increased attraction leads to a greater decrease in the mobility of $Ni^{2+}$ and $La^{3+}$ cations relative to their mobility in free solutions.

The passage from microporous 8V-NT glasses to macroporous ones leads to a commonly observed decrease in the $n_+$ values caused by a rise in the pore channel sizes, which is accompanied by a decrease in the degree of EDL overlapping and an increase in the coion concentration in the pore space. The selectivity of MAP membranes in the most diluted solution is rather high, $n_+ = 0.91 \pm 0.4$, because the electrokinetic radii are in a range of 0.18–0.28, and the degree of EDL overlapping remains high. Note that, for macroporous 8V-NT glasses, the pores of which contain no finely dispersed secondary silica, the $n_+$ values are close to each other for all three electrolytes at $C > 3.2 \times 10^{-4}$ g-equiv/L. At lower concentrations, the effect of electrostatic interaction of ions with the surface on their mobility diminishes because of a decrease in absolute value $|\sigma_0|$ of the surface charge, thereby leading to a slight increase in the $n_+$ values for nickel and lanthanum ions relative to sodium ions. In the case of iron-containing Fe-4-5 PGs, surface charge $|\sigma_0|$ of which is higher than that of 8V-NT [11], a decrease in the mobility of lanthanum ions in the MIP membrane is so great that the $n_+$ values at a pore radius of 3–3.4 nm become lower than those in the MAP membrane with pore radii of 17–19 nm (Fig. 2, dependences *2, 3*).

It should also be noted that, in the most concentrated solutions, when the surface charge has the maximum absolute value, a decrease in the mobility of the multivalent ions in the pore liquid for all studied membranes leads to the fact that the transport numbers of

$Ni^{2+}$ and $La^{3+}$ ions become lower than those in the corresponding free solutions, with this effect being unobserved for $Na^+$ ions.

The dependences of the transport numbers on electrolyte solution ionic strength $I$ for the studied cations are presented in Figs. 3 and 4. These dependences enable one to compare the transport properties of the membrane systems under the conditions of constant diffusion layer thickness $\delta = 1/\kappa$, i.e., at the same degree of EDL overlapping in all electrolytes. It is seen that, at $I = $ const, the values of $n_+$ coincide for $Na^+$ and $La^{3+}$ cations in 8V-NT MIP membrane, while the transport number for $Ni^{2+}$ is somewhat lower (Fig. 3, dependences *1–3*). Previous studies have shown that the surface charge of MIP glasses in electrolytes containing counterions with different charge values at $I = $ const is also almost constant [23]. Therefore, the main factors affecting the transport numbers seem to be a decrease in the mobility of counterions in secondary silica-containing pores and the electrostatic interaction of counterions having different charge values with the surface at a constant $|\sigma_0|$ value.

At the same surface charges and degrees of EDL overlapping, the character of the dependence of the transport number on the cation charge for 8V-NT MIP glasses becomes close to that observed in free solutions (Fig. 3). Specific features relevant to the ion transport in charged membranes manifest themselves at $I \leq 3 \times 10^{-3}$ M; e.g., the transport numbers of $Ni^{2+}$ and $La^{3+}$ ions become almost equal (Fig. 3, dependences *4–6*). The data obtained lead us to conclude that, at the same EDL structure in the pore space, the presence (or absence) of secondary silica in the pore channels has the main influence on the mobility and transport number of counterions in addition to the surface charge, which governs the numbers of co- and counterions in the pores.

The results of determining the $n_+$ values in iron-containing membranes at a constant ionic strength have shown that an increase in the surface charge decreases the mobility of trivalent cations in a manner such that the transport numbers of lanthanum ions in MIP glasses become equal to the transport numbers of sodium ions in MAP grasses (Fig. 3, dependences *2, 3*).

Figures 5 and 6 show the dependences of the transport numbers of $Na^{2+}$ and $La^{3+}$ ions on the ionic strength of electrolyte solutions for micro- and macroporous glasses with different compositions. It has appeared that, at a constant ionic strength and close values of the average pore radius (2–2.5 nm and 2.5–3 nm for 8V-NT MIP and Fe-4-5 MIP, respectively), the composition of a MIP glass has almost no effect on the transport number of sodium ions (Fig. 5, dependences *1, 3*). The transport numbers of $La^{3+}$ ions in Fe-4-5 MIP glass are lower than those in 8V-NT MIP glass (Fig. 6, dependences *1, 3*), thereby confirming

the assumption proposed in [12] about different structures of secondary silica in the pores of membranes containing magnetite and free of it. An increase in the surface charge and a decrease the sizes of the pore channels in Fe-4-5 MAP glass lead to higher transport numbers of $Na^+$ and $La^{3+}$ ions as compared with those in 8V-NT MAP glass (Figs. 5, 6; dependences *2, 4*).

## CONCLUSIONS

The influence of the charges of counterions on their transport numbers ($n_+$) in the pore channels of micro- and macroporous glasses with different compositions has been studied by the examples of sodium, nickel, and lanthanum cations (in the presence of the same coion, $Cl^-$). Classical regularities have been observed for each electrolyte: an increase in the concentration of an equilibrium solution and the sizes of the pore channels at a constant glass composition leads to a decrease in the values of $n_+$ due to a diminish in the contribution of EDL ions to the transport processes. In the most diluted solutions with ionic strength $I = 10^{-4}$ M, both macroporous and microporous membranes exhibit a high selectivity—the values of $n_+$ lie in a range of $0.87-1.0$. It should be noted that, in the case of the most concentrated solutions ($I \geq 0.1$ M), the transport numbers of multivalent $Ni^{2+}$ and $La^{3+}$ cations are lower than those in corresponding free solutions, with this effect being unobserved for sodium chloride.

The analysis of the data obtained has shown that the relation between the transport numbers of the counterions in this or that microporous glass is governed by the influence of the structure of secondary silica located in the pores on the ion mobility. This influence manifests itself both at a constant ionic strength, which ensures the same values of the surface charge and the degrees of EDL overlapping in different electrolytes, and at a variable EDL structure under the conditions of a constant equivalent solution concentration. For macroporous glasses, the pores of which contain no secondary silica, the ratio between the $n_+$ values becomes close to that observed in free electrolyte solutions at $I < 0.1$ M. Microporous glass composition has almost no effect on the transport number of sodium counterions at a constant ionic strength (the same degree of EDL overlapping in the pore channels). At the same time, the transport numbers of lanthanum counterions are lower in iron-containing Fe-4-5 MIP glass than in 8V MIP glass because of different structures of the secondary silica in these porous glasses.

## ACKNOWLEDGMENTS

## FUNDING

## CONFLICT OF INTEREST

The authors declare that they have no conflict of interest.

## REFERENCES

1. Mazurin, O.V., Roskova, G.P., Aver'yanov, V.I., and Antropova, T.V., *Dvukhfaznye stekla: Struktura, svoistva, primenenie* (Biphasic Glasses: Structure, Properties, and Application), Leningrad: Nauka, 1991.

2. Yairi, M. and Richter, C., *Sens. Actuators, A,* 2007, vol. 137, p. 350.

3. Evstrapov, A.A., Esikova, N.A., Rudnitskaja, G.E., and Antropova, T.V., *Opt. Appl.,* 2008, vol. 38, p. 31.

4. He, F., Liao, Y., Lin, J., Song, J., Qiao, L., Cheng, Y., and Sugioka, K., *Sensors* (Basel), 2014, vol. 14, p. 19402.

5. Zakoldaev, R.A., Sergeev, M.M., Sivers, A.N., Danilov, P.A., Veiko, V.P., Kudryashov, S.I., Kostyuk, G.K., Ionin, A.A., Anfimova, I.N., and Antropova, T.V., *Glass Phys. Chem.,* 2018, vol. 44, p. 486.

6. Andreeva, Y.M., Sergeev, M.M., Zakoldaev, R.A., Gabysheva, U.E., Veiko, V.P., Kudryashov, S.I., Ionin, A.A., Vocanson, F., Itina, T.E., Antropova, T.V., and Medvedev, O.S., *J. Laser Micro/Nanoeng.,* 2018, vol. 13, p. 193.

7. Veiko, V.P., Zakoldaev, R.A., Sergeev, M.M., Danilov, P.A., Kudryashov, S.I., Kostiuk, G.K., Sivers, A.N., Ionin, A.A., Antropova, T.V., and Medvedev, O.S., *Opt. Express,* 2018, vol. 26, p. 28152.

8. Volkova, A.V., Ermakova, L.E., Kashpurina, E.A., Pshenko, O.A., and Antropova, T.V., *Glass Phys. Chem.,* 2016, vol. 42, p. 322.

9. Ermakova, L.E., Grinkevich, E.A., Volkova, A.V., and Antropova, T.V., *Colloid J.,* 2018, vol. 80, p. 492.

10. Ermakova, L.E., Antropova, T.V., Volkova, A.V., Kuznetsova, A.S., Grinkevich, E.A., and Anfimova, I.N., *Glass Phys. Chem.,* 2018, vol. 44, p. 269.

11. Ermakova, L.E., Grinkevich, E.A., Volkova, A.V., Kuznetsova, A.S., Kurilenko, L.N., and Antropova, T.V., *Colloid J.,* 2019, vol. 81, p. 235.

12. Ermakova, L.E., Kuznetsova, A.S., Antropova, T.V., Volkova, A.V., and Anfimova, I.N., *Colloid J.,* 2020, vol. 82, p. 262.

13. Helfferich, F.G., *Ionenaustauscher,* Weinheim: Verlag Chemie, 1959.

14. Gerasimov, Ya.I., Dreving, V.P., Eremin, E.N., et al., *Kurs fizicheskoi khimii* (Course of Physical Chemistry), Moscow: Khimiya, 1973, vol. 2.

15. *Spravochnik po elektrokhimii* (Handbook of Electro-chemistry), Sukhotin, A.M., Ed., Leningrad: Khimiya, 1981.

16. Grigorov, O.N., Koz'mina, Z.P., Markovich, A.V., and Fridrikhsberg, D.A., *Elektrokineticheskie svoistva kapil-lyarnykh sistem* (Electrokinetic Properties of Capillary Systems), Moscow: Akad. Nauk SSSR, 1956.

17. Lidin, R.A., Andreeva, L.L., and Molochko, V.A., *Konstanty neorganicheskikh veshchestv: Spravochnik* (Constants of Inorganic Substances: Handbook), Mos-cow: Drofa, 2006.

18. *Spravochnik khimika* (Chemist's Handbook), Ni-kol'skii, B.P., Ed., Moscow: Khimiya, 1966, vol. 1.

19. Shannon, R.D. and Prewitt, C.T., *Acta Crystallogr. B,* 1969, vol. 25, p. 925.

20. *Spravochnik khimika* (Chemist's Handbook), Ni-kol'skii, B.P., Ed., Moscow: Khimiya, 1965, vol. 3.

21. Robinson, R.A. and Stokes, R.H., *Electrolyte Solutions,* Butterworths Sci. Publ., 1955.

22. Ermakova, L.E. and Volkova, A.V., *Colloid J.,* 2017, vol. 79, p. 459.

23. Ermakova, L.E., Electrosurface phenomena in nano-dispersed systems, *Doctoral (Chem.) Dissertation,* St. Petersburg: St. Petersburg State Univ., 2001.

*Translated by A. Kirilin*